SUB-SYSTEM TESTS FOR ASSESSING PEDESTRIAN PROTECTION BASED ON COMPUTER SIMULATIONS

E.G. Janssen and J.J. Nieboer
TNO Road-Vehicles Research Institute
Crash Safety Research Centre
Delft, The Netherlands

Abstract

EEVC Working Group 10 has developed test methods and acceptance levels for assessing the protection afforded to pedestrians by the fronts of cars in an accident. These methods include sub-system tests to the bumper, the bonnet leading-edge and the bonnet top. Computer simulations were used to define the impact mass, velocity, angle and location of the three sub-system tests.

In the framework of this EEVC research program, TNO performed a large number of computer simulations using the MADYMO CVS program. A 2-dimensional model of a pedestrian laterally impacted by the vehicle front has been used in the current study. Parameter variations are performed, aimed to show the influence of the vehicle's speed, shape and stiffness, as well as the influence of the pedestrian's anthropometry and walking position. The results of 63 simulations are analysed with respect to input test conditions of the bumper, the bonnet leading-edge and bonnet top, sub-system test and with respect to injury parameters. In this paper only the bonnet leading-edge impact results will be adressed. Special algorithms have been developed to calculate for instance the effective mass of the impact or the bending moments in the legs of a 50th percentile male, a 5th percentile female and a six-year-old child dummy. Based on the results of these simulations, test conditions for the sub-system tests on the leading-edge of a passenger car are proposed.

The paper describes the computer model set-up, the parameter variations, the special purpose algorithms and the simulation results in terms of input conditions for the pedestrian sub-system tests and associated injury criteria. The simulations indicate that the input conditions are strongly dependent on the vehicle's shape and less on the vehicle's stiffness.

Introduction

In most European countries, unprotected road users account for a significant proportion of the road accident casualties. In almost every country, pedestrians are the most frequently involved. In the past years international research was focussed mainly on pedestrian safety. Based on this research various recommendations for the front structure design of passenger cars were developed. Moreover, test methods and regulations have been proposed to assess pedestrian protection.

In the Spring of 1987 one of these proposals [1]* was discussed by the EEC ad-hoc working group 'Erga Safety'. It was concluded that the basis of the proposal was promising, however,

* Numbers in brackets designate references at the end of the paper.

limited additional research was needed to fill up some white gaps. The European Experimental Vehicles Committee (EEVC) was asked to coordinate this research and at the end of 1987 EEVC Working Group 10 was set up. The mandate of the group was 'to determine test methods and acceptance levels for assessing the protection afforded to pedestrians by the fronts of cars in an accident'. The test methods should be based on sub-system tests, essentially to the bumper, bonnet leading-edge and bonnet top surface. The different impact characteristics associated with changes in the general shape of the car front should be allowed for by variations in the test conditions (e.g. impactor mass, velocity, direction of impact). The test conditions should be based on full scale test data and computer simulations. Assessment for compatibility with other existing regulations should be performed.

The work was shared between five laboratories: TRRL (UK), BASt (FRG), APR (Fr.), INRETS (Fr.) and TNO (NL). TNO's task was to evaluate the three sub-system tests developed by the other labs, to contribute to the compatibility study and to perform the computer simulations used to define the sub-system input conditions.

The current paper summarizes the computer simulations performed by TNO in the framework of the EEVC WG10 research program. The paper describes the MADYMO CVS model set-up, the parameter variations and the simulation results in terms of input conditions for the pedestrian sub-system tests and associated injury criteria. The presentation of the results is limited to the bonnet leading-edge impact.

Computer simulations

General model set-up

The development of the Crash Victim Simulation program MADYMO started in the mid-seventies. The program performs time-history simulations for an arbitrary number of systems of rigid bodies in either two- or three-dimensional inertial space. The rigid bodies can be connected by hinge joints (2D) or ball and socket joints (3D). Each of the bodies may be in force interaction with any of the other bodies or with its surroundings. The program automatically generates and solves the set of non-linear equations of motion. Special force-interaction modules have been developed, making the program particularly suitable for crash analysis [2, 3]. Version 4.2 of MADYMO 2D is used for this pedestrian protection research program.

Figure 1 shows the applied model set-up; a pedestrian is impacted laterally by the front of a passenger car. The car front is modelled in MADYMO by a null system [3], having a prescribed horizontal velocity. Both spoiler and bumper are represented by an ellipse in this system. The grill and the bonnet are represented by planes connected by a circle shaped leading-edge. By varying the bumper height, bumper lead and bonnet leading-edge height, different car types can be simulated. In Figure 1 the so-called standard car geometry is illustrated. An equal stiffness, is specified for all vehicle elements. This base stiffness K (i.e. a maximum force level of 4000 N) is based on computer simulations performed by Harris and Grew [4]. The vehicle impact speed is 40 km/h and the vehicle is not braking.

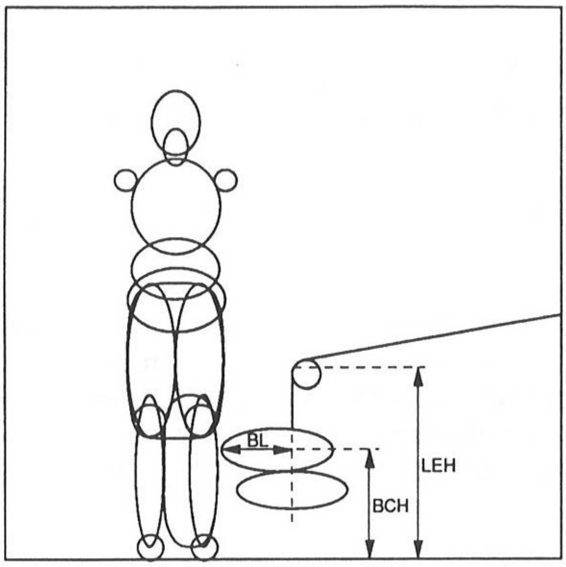

Figure 1 *Model set-up showing a 50^{th} percentile male and standard vehicle dimensions (Bumper Centre Height = 390 mm, Bumper Lead = 225 mm, Leading-edge Height = 700 mm).*

A 50^{th} percentile male dummy, a 5^{th} percentile female dummy and a six-year-old child dummy are simulated. Only a 50^{th} percentile male dummy database already existed as part of the MADYMO databases [5]. The characteristics for elastic bending in the neck and the knees were adjusted in this database in order to obtain a more human-like dummy behaviour. The 5^{th} percentile female database was derived from the 50^{th} percentile database by means of scaling techniques [6], except for the hip joint characteristics. The six-year-old child database was derived from a three-dimensional in-house database of the TNO P6 dummy. In the 50^{th} percentile male, 5^{th} percentile female and six-year-old child databases a linear rotational stiffness in the knee joints is specified of 716, 700 and 500 Nm/rad respectively. Figure 2 shows the model set-up of the three dummy databases used. As can be seen from this figure, second ellipses with larger dimensions have been attached to the upper and lower left legs for defining contact interaction. This was necessary because vehicle-leg penetration appeared to be large as compared with the original leg ellipse dimensions. The legs are placed in a 'walking position', which means no contact between the legs is defined.

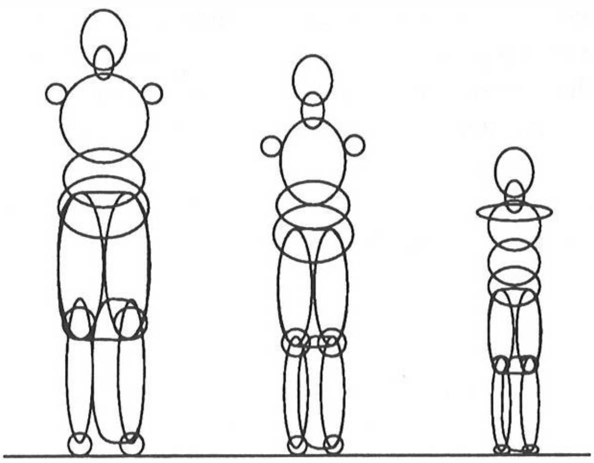

Figure 2 *Pedestrian databases; 50^{th} percentile male dummy, 5^{th} percentile female dummy and six-year-old child dummy.*

Special purpose algorithms

Important results as maximum accelerations, forces on body parts, maximum knee bending angles and some other injury criteria follow directly from a MADYMO simulation. Special algorithms (i.e. user-defined modules and post-processing programs) had to be developed to calculate for instance the normal impact velocity of body parts against a vehicle, the deformation energy absorbed by the impact, the effective masses of the impacting body parts and maximum bending moments in the legs.

One of these programs calculates data concerning all dummy contacts with the car exterior. The data are specified for the time of first contact and the time of maximum penetration. It includes penetration, normal and tangential impact velocity, impact angle "α" and orientation angle "β". See Figure 3 for an illustration of these angles for a leading-edge impact situation. For the analysis of the simulations only the total impact angle "γ" was taken into account. This angle is defined as follows:

$$\gamma = \alpha + \beta - 90 \qquad (1)$$

In addition the impact location is calculated in the coordinate system of the passenger car and the local coordinate system of the contacting dummy element.

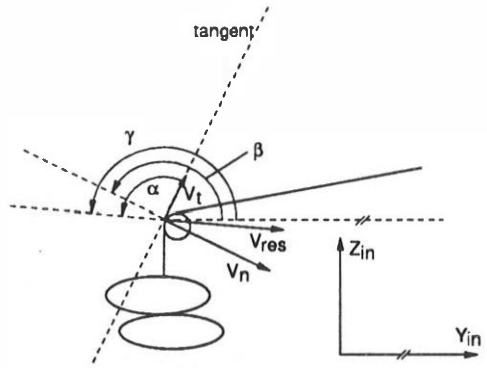

Figure 3 Definition of output data for leading-edge impact.

A second program calculates the maximum and minimum bending moments occurring in the upper or lower leg elements of the dummy. The magnitude of the bending moment is considered here to be an indication of the severity of possible leg injuries. For the calculation it is assumed that the largest bending moment will occur at the intersection where the largest contact force is applied to the element. Furthermore, it is assumed here that no external forces are applied to the element in between the location of the bending moment calculation and the end of the element. For the magnitude of the bending moments inertia effects are taken into account.

A third program calculates the deformation energy (E) absorbed by the impact per specified contact interaction in the MADYMO input dataset. For this calculation only the elastic part of the contact force is taken into account. If the normal impact velocity is known, the effective mass of the impacting body is defined as:

$$m_{eff} = 2E / v_n^2 \qquad (2)$$

Parameter variations

The computer simulation work has been divided into two phases. The first phase consists of 15 simulations with each of the three pedestrian datasets (i.e. 50^{th} percentile male dummy, 5^{th} percentile female dummy and six-year-old child dummy), in which the bumper centre height, the bumper lead and bonnet leading-edge height are varied (see Table 1). A combination of vehicle dimensions is chosen here to correspond with current styles of cars and possible future trends. The bumper vertical depth is always 100 mm in these simulations. The general model set-up described in the previous section is applied here. With these 45 basic simulations the influence of the vehicle geometry and pedestrian anthropometry can be identified. In the second phase 18 additional simulations have been performed in order to analyse the influence of the vehicle impact speed, the vehicle stiffness and the standing position of the pedestrian. For a standard car geometry (simulation no. 1 in Table 1) and for all three pedestrian sizes, simulations were conducted with a vehicle velocity of 30 km/h rather than 40 km/h. To evaluate the influence of vehicles stiffness on the pedestrian kinematics and injuries, the vehicle stiffness has been varied as well in this study (see Figure 4).

no.	Leading-edge height (mm)	Bumper lead (mm)	Bumper center height (mm)	Vehicle front angle (°)
1	700	225	390	51
2	700	225	330	56
3	700	225	450	44
4	700	100	330	73
5	700	100	390	70
6	700	100	450	65
7	700	350	330	44
8	700	350	390	38
9	700	350	450	32
10	600	225	390	38
11	600	100	390	60
12	600	350	390	26
13	800	100	390	75
14	800	225	390	59
15	800	350	390	47

Table 1 Variation in vehicle dimensions (see also Figure 1).

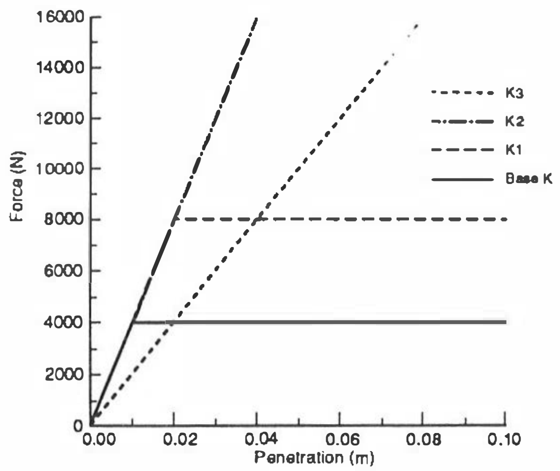

Figure 4 *Car exterior stiffness variations.*

The leg position of the pedestrian influences the kinematics during the impact. A 'walking position', which means one leg forward and one leg backward, causes a rotation of the pedestrian around a vertical axis, avoiding shoulder contact and showing a direct head-to-bonnet impact. In a 2D simulation this rotation is not possible. To analyse the influence of leg position and shoulder contact, these parameter variations have been included in the simulations. In the 'walking position' no contact between both legs is defined in the 2D model, while in the 'standing position' the legs are parallel to each other and leg-to-leg contact is prescribed.

Table 2 shows the complete simulation program. The vehicle velocity, shoulder contact and leg position, the vehicle stiffness and the pedestrian size are shown for the 45 basic simulations (i.e. vehicle shape variations) and the 18 additional simulations.

30 km/h		40 km/h					
Shoulder contact Walking position		Shoulder contact Walking position				No shoulder contact Walking position	Shoulder contact Standing position
Stiffness	Base K	Base K	K1	K2	K3	Base K	Base K
50th %ile Male	1	15 shape variations	1	1	1	1	1
5th %ile Female	1	15 shape variations	1	1	1	1	1
6y child	1	15 shape variations	1	1	1	1	1

Table 2 *Summary of model set-up of 45 basic and 18 additional simulations.*

Results

Introduction

The results of the 45 basic and 18 additional simulations are presented separately in this section. To limit the length of this paper, not all simulation results are presented here, only the relevant results for the **bonnet leading-edge** impact.

A distinction is made between sub-system impact conditions (i.e. impact location, impact velocity, impact angle and effective impact mass) and injury criteria (e.g. bending moment). Figure 5 shows examples of the kinematics of the three pedestrians for the bonnet leading-edge impact.

Basic simulations

The relevant simulation results for the 50^{th} percentile male, 5^{th} percentile female and six-year-old child are summarized in Appendix 1. Only the bending moments in the left upper leg (i.e. impact side) of the adult pedestrians have been calculated, since the child's upper leg does not impact the leading-edge.

The impact **location** on the leading-edge is defined by an impact orientation angle "betha" (see Figure 3). Since the angles of all 45 simulations were between 109° and 180°, and because of the small radius of the leading-edge circle, the impact location is almost constant for all three pedestrian sizes.

Figures 6 up to 8 show the influence of the vehicle shape on the leading-edge impact velocity for all three pedestrians. In Appendix 1 the contacted body part is presented. It appears from these simulations that the impact **velocity** on the leading-edge is strongly influenced by the vehicle shape. In general, the impact velocity increases up to vehicle impact speed with a lower bumper centre height, a shorter bumper and a higher leading-edge (see Figures 6 up to 8). The leading-edge velocity reduces to less than 50% of the vehicle speed if the vehicle has a high, deep bumper and a low bonnet leading-edge.

Figure 9 shows the influence of the vehicle shape on the total impact **angle**. In case of the 50^{th} percentile male impact simulations, always the upper leg is impacted by the leading-edge. Therefore these results show a clear trend. The total impact angle appears to be 180° (i.e. horizontal and opposite to vehicle speed) with a short bumper lead (see Figure 9). The total impact angle decreases if the bumper lead increases or the leading-edge height decreases, and finally becomes 90° (i.e. a vertical impact). The range of impact angles for the child and female impact simulations appears to be similar to that of the male impacts.

The bumper lead and height hardly influence the **effective mass** in the child and female impacts (see Figure 11 and 12), however, they appear to have some influence in the male impacts (see Figure 10). A similar trend can be found with the influence of the leading-edge height; a large influence for the male impact only.

Maximum penetration and deformation energy are also presented in Appendix 1. In general, high penetration and energy absorption is found with high vehicle fronts and vice versa.

The influence of the pedestrian's **anthropometry** can be analyzed by comparing the responses for the same vehicle shape. It appears that the impact velocity, - location and - angle are always in the same range for the three pedestian sizes. However, for the effective mass considerable differences can be seen (see Figures 10 up to 12); for instance the effective masses for a BL225/BCH390/LEH800 mm vehicle shape are 20.2 kg (male), 10.3 kg (female) and 4.6 kg (child).

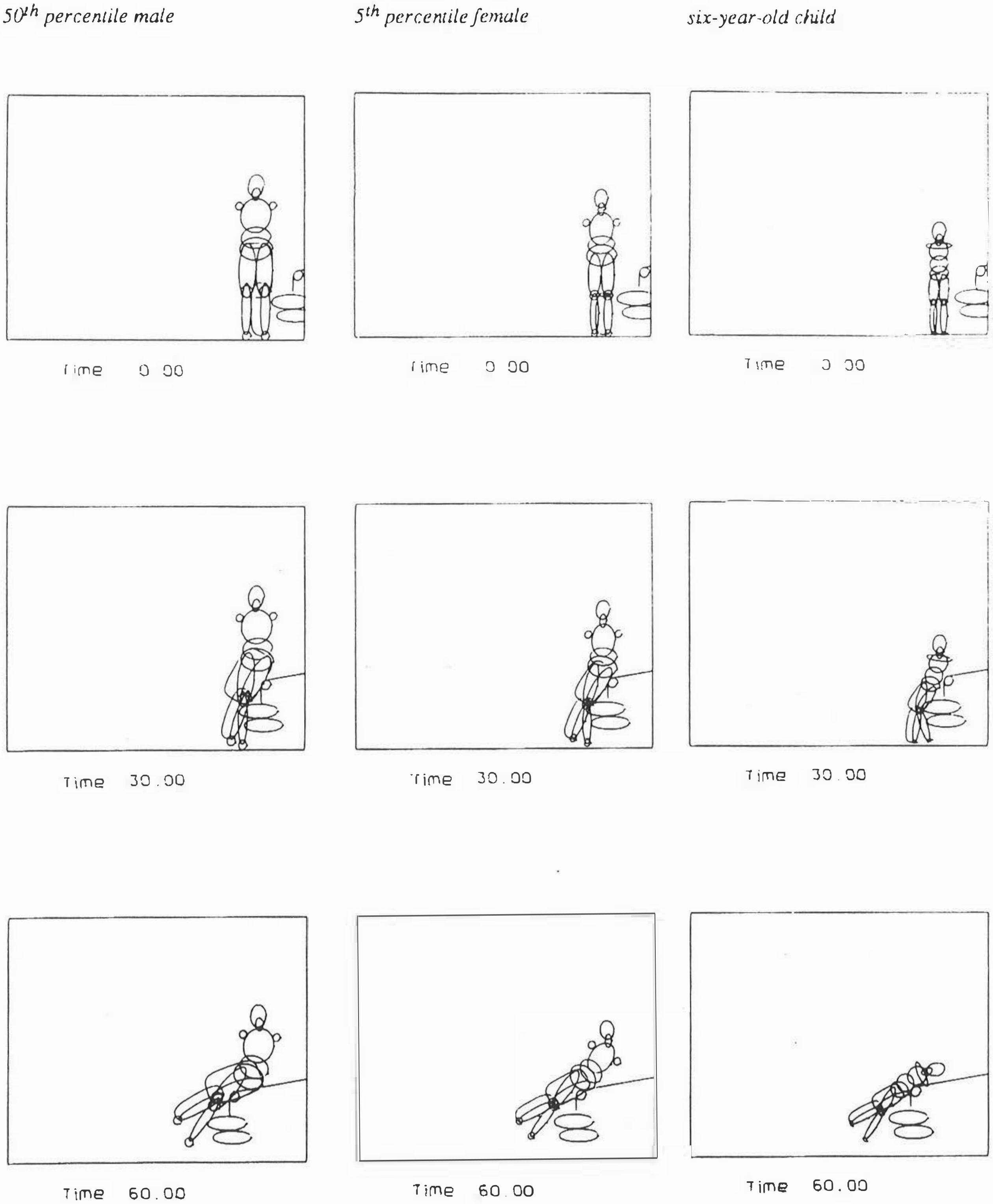

Figure 5 *Simulated kinematics of the 50^{th} percentile male, 5^{th} percentile female and six-year-old child dummy (40 km/h, basic car stiffness, shoulder-bonnet contact and no leg-leg contact).*

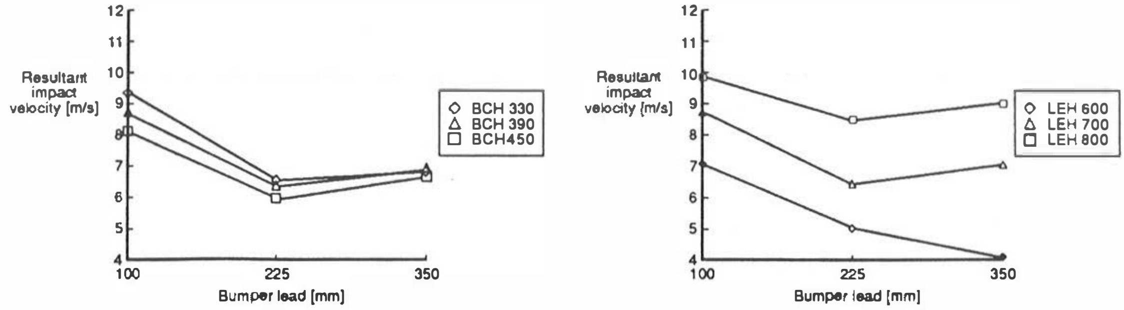

Figure 6 *Resultant impact velocity for 50^{th} percentile male in leading-edge impact (left: LEH = 700 mm, right: BCH = 390 mm).*

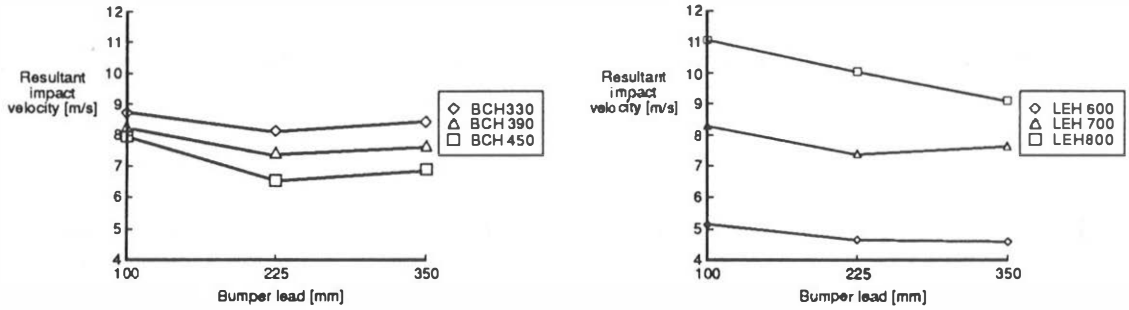

Figure 7 *Resultant impact velocity for 5^{th} percentile female in leading-edge impact (left: LEH = 700 mm, right: BCH = 390 mm).*

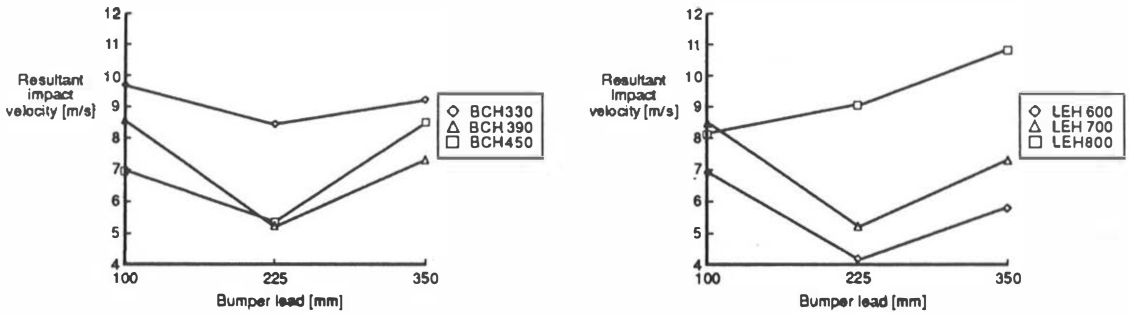

Figure 8 *Resultant impact velocity for six-year-old child in leading-edge impact (left: LEH = 700 mm, right: BCH = 390 mm).*

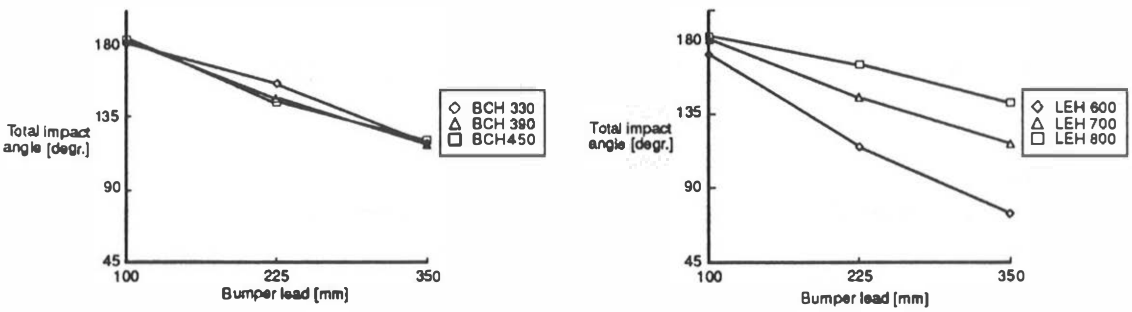

Figure 9 *Total impact angle for 50^{th} percentile male in leading-edge impact (left: LEH = 700 mm, right: BCH = 390 mm).*

In general the **bending moment** in the upper leg of the 50[th] percentile male and 5[th] percentile female increases when the bumper lead and/or the leading-edge height decreases. The bending moment in the female upper leg appears to be always (sometimes considerable) lower than that calculated for the male upper leg impacted by the same vehicle front.

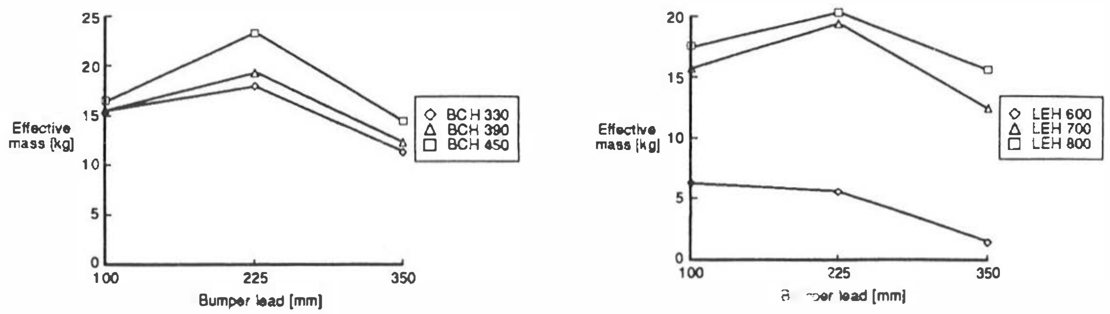

Figure 10 *Effective mass for 50[th] percentile male in leading-edge impact (left: LEH = 700 mm, right: BCH = 390 mm)).*

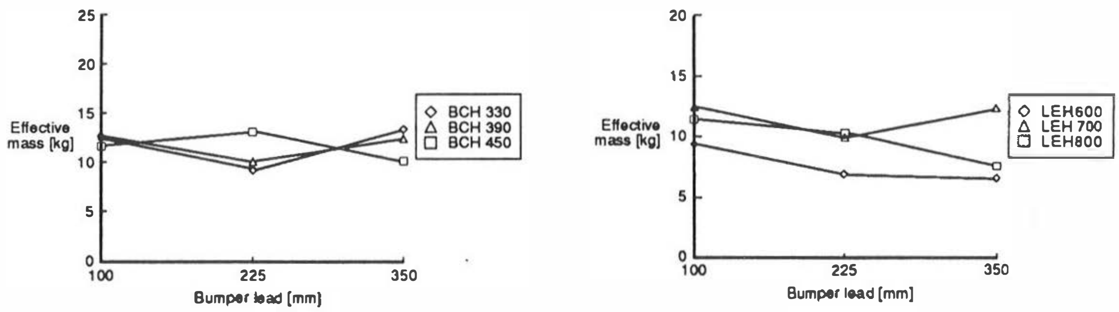

Figure 11 *Effective mass for 5[th] percentile female in leading-edge impact (left: LEH = 700 mm, right: BCH = 390 mm).*

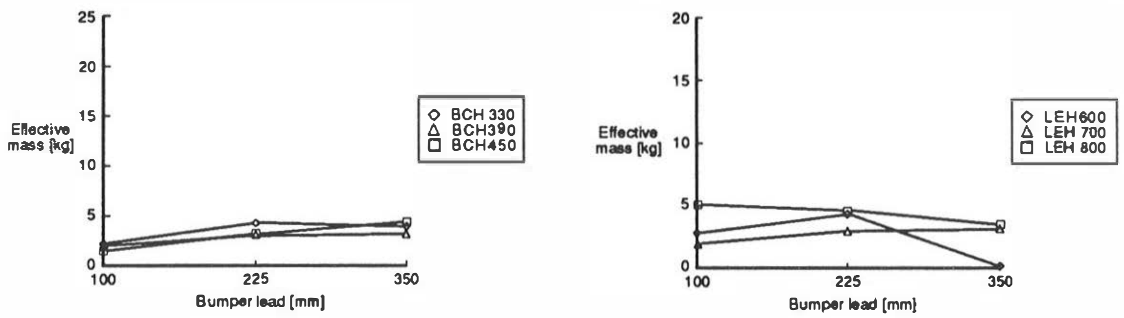

Figure 12 *Effective mass for six-year-old child in leading-edge impact (left: LEH = 700 mm, right: BCH = 390mm).*

Additional simulations

For leading-edge impacts the sub-system condition impact **location** is known. Impact angle, impact velocity and effective mass are to be varied. Figure 13 shows the resultant impact **velocity** as a function of the parameter variations shown in Table 2. As expected, the passenger car velocity influences the leading-edge impact velocity directly. The influence of car exterior stiffness on leading-edge impact velocity can be neglected, except for a stiffness change from Base K to K1 in case of a six-year-old child dummy. No influence of the contact interaction between shoulder and bonnet can be observed. A considerable influence can be seen for contact interaction between right and left leg for a 50[th] percentile male dummy.

Figure 14 shows the total impact **angle** as a function of the parameter variations performed (see Figure 3 for a definition of this angle). A slight influence of the vehicle speed on the impact angle for the adults can be seen, while the child shows a somewhat larger influence of the vehicle speed. An influence of vehicle exterior stiffness can be observed for both the 50th percentile male and the six-year-old child dummy. This influence is absent for the 5th percentile female dummy. Again there is no influence of the contact interaction between shoulder and bonnet. A minor influence can be observed for the interaction between right and left leg.

Figure 15 shows the effective mass as a function of the parameter variations. The passenger car velocity influences only the **effective mass** in case of a 50th percentile male dummy. For all three dummy types the effective mass is affected by the vehicle exterior stiffness. There is no influence of the contact interaction between shoulder and bonnet. A relatively large influence was found for the contact interaction between right and left leg for both a 50th percentile male and a six-year-old child dummy.

For leading-edge impact the maximum **bending moment** in the upper leg is considered to be an injury criterion for the 50th percentile male and 5th percentile female dummies. When simulating a six-year-old child dummy, the leading-edge of the standard car first contacts the spine ellipse of the dummy. No injury criterion for the abdomen/spine region has been taken into consideration here. Figure 16 shows the maximum bending moment as a function of the parameters varied. As can be seen in this figure the maximum bending moment is not very sensitive for vehicle velocity. A larger influence can be observed for the car exterior stiffness, the latter influence is large for a 50th percentile dummy. There is no influence of the contact interaction between shoulder and bonnet, while a considerable influence can be seen for the interaction between right and left leg.

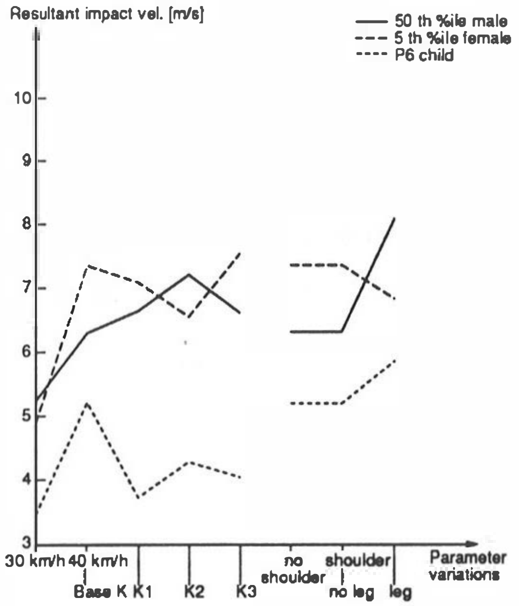

Figure 13
Resultant impact velocity for bonnet leading-edge impact as function of parameter variations.

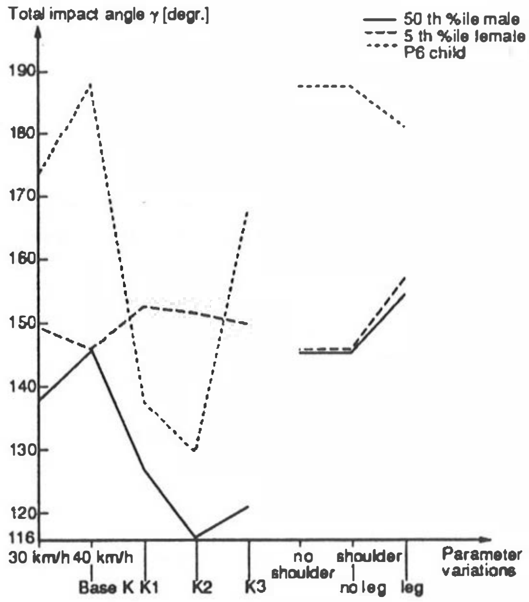

Figuur 14
Total impact angle for bonnet leading-edge impact as function of parameter variations.

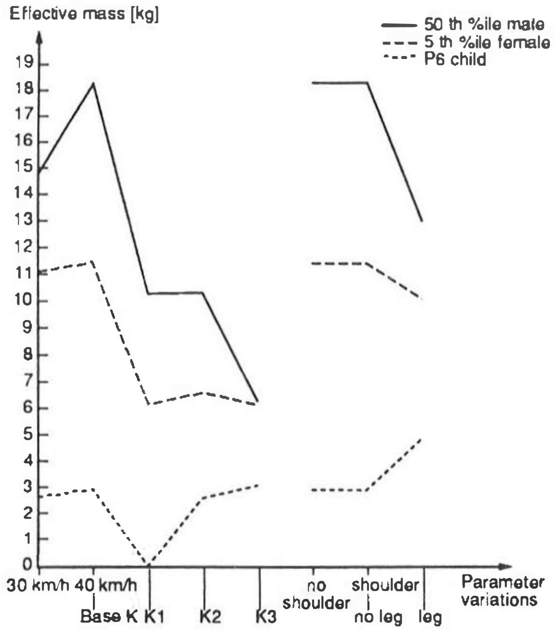

Figure 15
Effective mass for bonnet leading-edge impact as function of parameter variations.

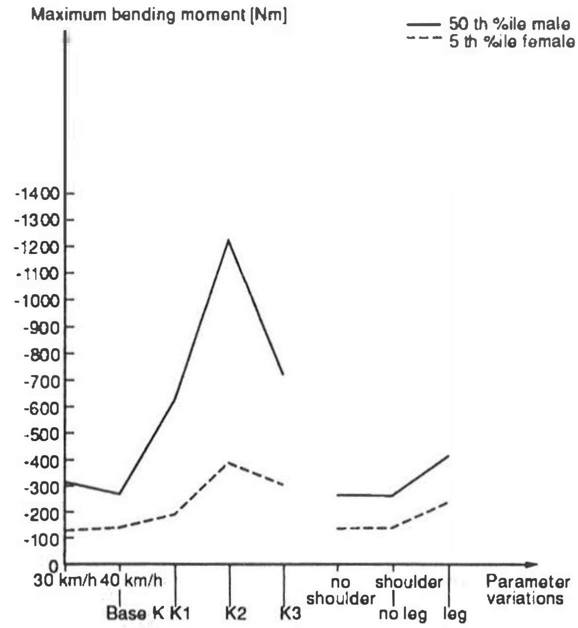

Figure 16
Maximum bending moment for bonnet leading-edge impact as function of parameter variations.

Sub-system test specifications

Introduction

In this section the simulation results are summarized and discussed. Based on these general conclusions test specifications for the leading-edge sub-system impact are proposed.

Discussion of the simulation results

The results of the 45 basic simulations with respect to the leading-edge impact are summarized in Table 3. This table shows the ranges of the impact conditions and protection criteria.

Leading-edge impact Parameter	range 50th perc. male	range 5th perc. female	range 6y child
impact velocity (m/s)	4.0 - 9.8	4.6 - 11.1	4.2 - 10.8
impact angle (degr.)	74 - 182	84 - 181	64 - 188
effective mass (kg)	1.3 - 23.3	6.6 - 13.3	0 - 5.1
max. penetr. (mm)	11 - 183	23 - 111	14 - 55
def. energy (J)	5 - 842	54 - 502	0 - 192
max. bending mom. (Nm)	161 - 942	127 - 510	-

Table 3 *Summary leading-edge impact basic simulations.*

The impact velocity, - location and - angle of a leading-edge sub-system test appear to be in the same range for all three pedestrian sizes. For the effective mass, two ranges would be necessary; a large mass representing an adult upper leg and a small mass representing a child torso (e.g. abdomen). Furthermore, the stiffness of these impactor faces would be different. A sub-system test method representing an adult upper leg impact only (i.e. 50th percentile male) is proposed here. Accident statistics should indicate the need for a child sub-system test on the bonnet leading-edge.

It has to be noted here that the results of the six-year-old child appear to be influenced by the shape of the contact ellipses (see also Figure 2). Since the outer contour of the pedestrian is not a smooth, more or less straight line, but consists of a number of circles and ellipses, the interaction with the leading-edge circle is non-linear in terms of impact location, impact angle and impact velocity. The results presented for the six-year-old child should be regarded with great care in this respect.
Furthermore the child contacts the whole vehicle front, including grill and bonnet, and not only the leading-edge. The lower torso, for instance can contact the grill before contacting the leading-edge. This influences the calculated deformation energy absorbed by the leading-edge and therefore influences the effective mass. It was decided to include the deformation energy of these additional contacts in the leading-edge contact.

The maximum bending moment in the upper leg can be used as an injury criterion. A good distinction is made between the different vehicle exterior stiffnesses by this criterion. The vehicle speed seems to have no influence on the bending moments (see also Figure 16). No injury criterion was available for the child's torso.

Most simulations have been performed with a vehicle impact speed of 40 km/h. It appears that decreasing this speed to 30 km/h, strongly influences the impact velocity on the leading-edge (e.g. -20% for 50^{th} percentile male and -50% for 5^{th} percentile female). EEVC Working Group 10 decided to define a vehicle impact speed of 40 km/h.

It was also decided (see 'Introduction') to base the input test conditions on the shape of the vehicle and not on the stiffness. The latter would require an integrated test method in which the results of the first test (i.e. bumper impact) would influence the test conditions of the second test (i.e. the leading-edge impact). Mathematical model simulations could be used in this integrated approach.
The stiffness of the vehicle also influences the shape (i.e. penetration) during the impact. This could influence the test conditions of the sub-system tests. For instance, it was found that for a relatively stiff bumper somewhat smaller impact angles (i.e. -20%) on the leading-edge are required in case of the 50^{th} percentile male impact (see Figure 3 for definition of the total impact angle). The influence of the bumper stiffness on the leading-edge impact velocity appears to be minor. The stiffness of the impacted vehicle part influences (of course) the effective mass of the impact on that part. For a relatively stiff vehicle exterior the effective mass is lower than for a relatively soft vehicle exterior. The vehicle stiffness also strongly influences the protection criteria responses, which is important to discriminate between 'good' and 'bad' vehicles with respect to pedestrian protection.

The leg position of the pedestrian, 'standing' or 'walking' position, influences the kinematics during the impact. A walking position, which means one leg forward and one leg backward, causes two impacts between bumper and legs. These impacts are separated in time and place. A standing position, which means the legs parallel to each other, results in one impact between bumper and leg, shortly followed by a leg-to-leg impact. A walking position shows (in these 2D simulations):

- a lower impact velocity in the leading-edge impact (e.g. -25% for the 50th percentile male);
- a higher effective mass for the adult pedestrian (e.g. +30% for the 50th percentile male) and a lower effective mass for the child pedestrian in the leading-edge impact;
- a slight influence on the bending moments for the adult pedestrian in a leading-edge impact.

Most simulations were performed with the pedestrian in walking position, where the responses of the leg at the impact side show higher values than those at the non-impact side.

Bonnet leading-edge test specifications

Based on the computer simulations described in the previous section, input test conditions for the sub-system test method are proposed. The proposal is based on a vehicle impact speed of 40 km/h (chosen by EEVC WG 10) and on a 'walking' position of the pedestrian. The latter means that a somewhat lower impact velocity and higher effective mass is necessary compared with a 'standing position'.

The proposed test specifications for the sub-system leading-edge impact are (50th percentile male only):

- impact velocity : variable (see Figure 17)
- impact location : 'leading-edge'
- impact angle : variable (see Figure 18)
- impact mass : variable (see Figure 19).

EEVC Working Group 10 has defined methods to identify the location and dimensions of the 'bumper' and 'leading-edge'. Based on these measurements the input conditions for a sub-system test on the bonnet leading-edge can be found from above presented specifications.
Figure 20 illustrates an adult upper leg impact against a bonnet leading-edge. As mentioned before accident statistics should indicate the need for a second sub-system test, representing a child's abdomen.

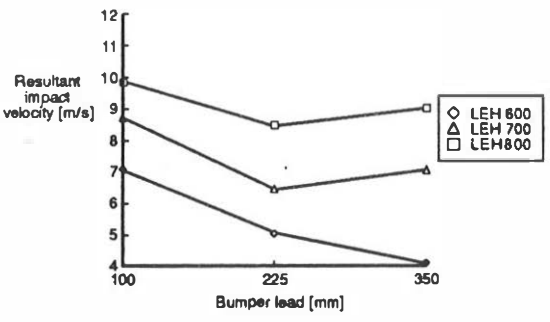

Figure 17
Proposed impact velocity for 50th percentile male in leading-edge test.

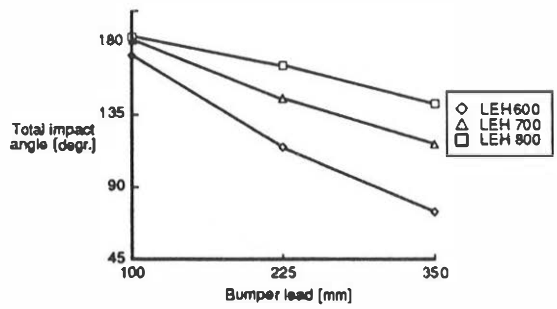

Figure 18
Proposed impact angle for 50th percentile male in leading-edge test.

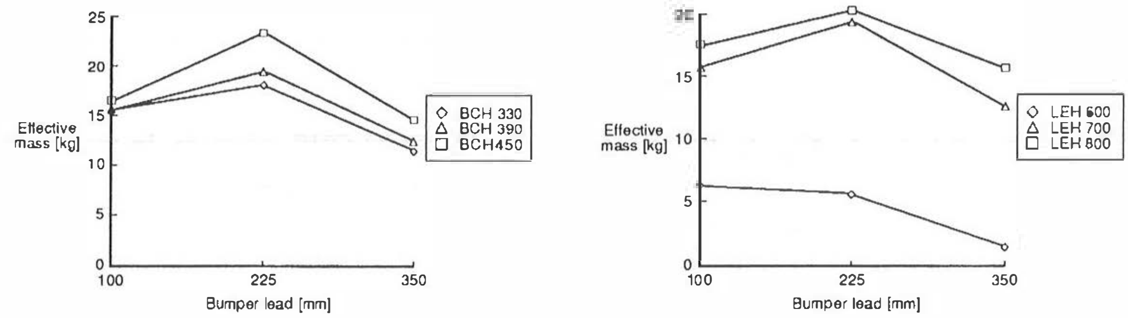

Figure 19 *Proposed impact mass for 50^{th} percentile male in leading-edge test (left: **LEH** = 700 mm, right: BCH = 390 mm).*

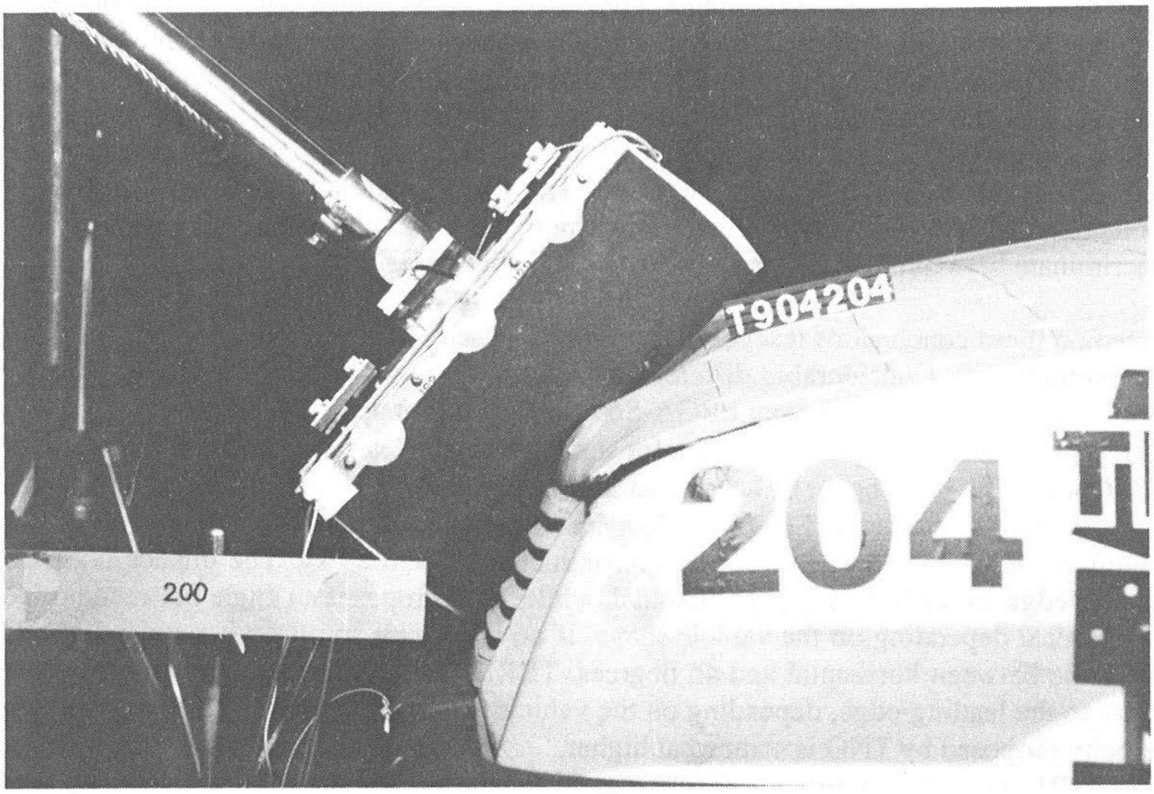

Figure 20 *Leading-edge sub-system impactor, representing an adult upper leg, developed by TRRL.*

Discussion and conclusions

In the previous EEVC reports dealing with pedestrian safety [7, 8], the value of mathematical models especially in combination with component or sub-system testing has been well recognised. Computer simulation models have been extensively used to obtain a better understanding of the interactions in an impact between a pedestrian and a vehicle and of the influence that changes in cars frontal shape would have on these interactions [4, 9, 10].
Based on the results of simulations using the Calspan CVS program, TRRL (UK) proposed a test method using sub-system testing for evaluating pedestrian protection for passenger cars. This document [1] was used as a basis for the research programme of EEVC Working Group 10. Test conditions for the sub-system tests on the bumper, bonnet leading-edge and bonnet

top are proposed. To support this existing data, further simulations are undertaken using a different model to give a broader set of data and a more comprehensive validation.

This additional validation is done by TNO using the MADYMO CVS program. In the past it was shown that relatively simple 2-dimensional models offer satisfactory results compared with results obtained from a 3-dimensional simulation [11]. Disadvantages of the application of 3D models are the increase in computer run time and input parameters, as well as the complexity of necessary contact models and special new algorithms. It was concluded in [11] that the use of 2D models is advisable in many cases. Version 4.2 of MADYMO 2D has been used in the current research program. Special emphasis is given to the rotation of the pedestrian due to its leg position.

Only the results for the bonnet leading-edge impact are presented here. For the bumper and bonnet top impact results it is refered to [12]. From the 45 basic simulations and 18 additional simulations it was shown that some vehicle parameters considerably influence the pedestrian responses, while some parameters hardly influence these responses. Furthermore, it was shown that the responses of the 5th percentile female are within the ranges of responses of the 50th percentile male and six-year-old child. The simulations have shown that the selected protection criteria, for instance the bending moment in the upper leg, are very well able to discriminate between different vehicle shapes and stiffnesses.

Based on these conclusions test conditions are proposed for the sub-system tests on the bonnet leading-edge. Considerable differences between these proposals and the original TRRL proposals described in document ERGA-S60 [1] can be found.
TRRL proposed a 16 kg impact mass for the adult upper leg to leading-edge impact, while TNO proposes a mass between 1.3 and 23.3 kg depending on the vehicle shape. If no leading-edge impact on sportcars (i.e. a very low leading-edge and very large bumper lead) is required, the mass would vary between approximately 10 and 23 kg. The impact angle on the leading-edge, described by [1] is horizontal, while TNO proposes an angle between horizontal and vertical depending on the vehicle shape. If no impact on sportcars is required, the angle would be between horizontal and 45 degrees. TRRL and TNO are proposing an impact velocity to the leading-edge, depending on the vehicle shape (see Figure 21). It appears that the velocity proposed by TNO is somewhat higher.
The TRRL and TNO simulation results, together with the results from dummy and cadaver tests, have been integrated by EEVC Working Group 10 to achieve realistic sub-system test conditions [13].

Acknowledgements

This research program was sponsored by the Department of Transport of the Dutch Govemment and by the Commission of the European Communities. TRRL provided data for the computer simulations, which were performed by Mr. Van Oorschot and Mr. Koppens of the TNO Crash Safety Research Centre.

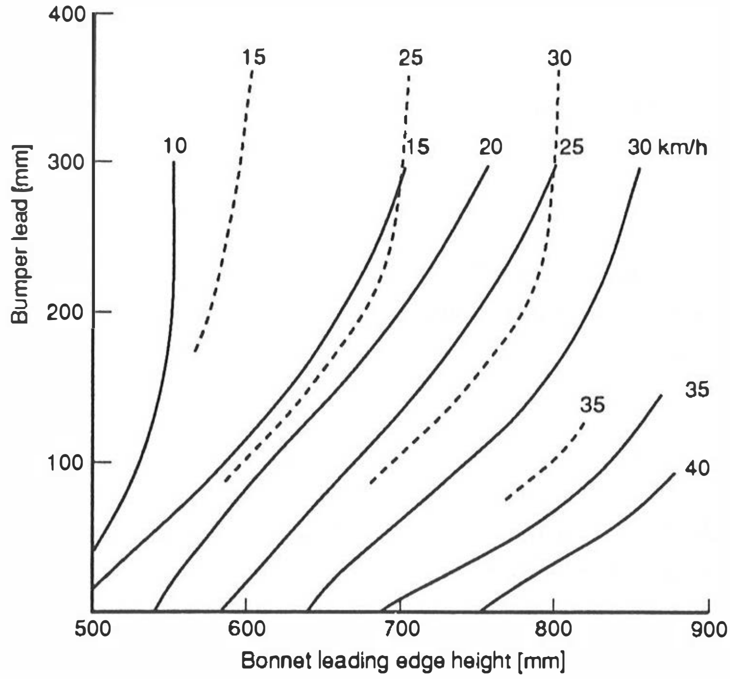

Figure 21 *Impact velocity for adult upper leg to leading-edge as proposed by TRRL (____) in reference [1] and as proposed by TNO (-----).*

References

1. Commission of the European Communities/Ad-hoc working group ERGA - Passive Safety/Document 60
   Frontal surfaces in the event of impact with a vulnerable road user.

2. H.A. Lupker, P.J.A. de Loo, J.J. Nieboer and J. Wismans
   Advances in MADYMO Crash Simulations.
   International Congres and Exposition, SAE 910879, Detroit, February 25-March 1, 1991.

3. MADYMO 2D User's Manual, Version 4.2
   TNO Road-Vehicles Research Institute, Delft, October 1988.

4. J. Harris and N.D. Grew
   The Influence of Car Design on Pedestrian Protection.
   Tenth International Technical Conference on Experimental Safety Vehicles,
   Oxford, July 1-4, 1985.

5. MADYMO Databases Manual, Version 4.2
   TNO Road-Vehicles Research Institute, Delft, October 1988.

6. H.J. Mertz, A.L. Irwin, J.W. Melvin, R.L. Stalnaker and M.S. Beebe
   Size, Weight and Biomechanical Impact Response Requirements for Adult
   Size Small Female and Large Male Dummies.
   International Congress and Exposition, SAE 890756,
   Detroit, February 27-March 3, 1989.

7. EEVC Committee
Pedestrian injury accidents.
Proceedings Ninth International Technical Conference on Experimental Safety Vehicles, Kyoto, Japan, November 1982.

8. EEVC Committee
Pedestrian injury protection by car design.
Tenth International Technical Conference on Experimental Safety Vehicles, Oxford, Great Britain, July 1985.

9. G.J.L. Lawrence
The influence of car shape on pedestrian impact energies and its application to sub-system tests.
Proceedings Twelfth International Technical Conference on Experimental Safety Vehicles, Gothenburg, Sweden, May 1989.

10. E.G. Janssen and J. Wismans
Experimental and mathematical simulation of pedestrian - vehicle and cyclist - vehicle accidents.
Proceedings Tenth International Technical Conference on Experimental Safety Vehicles, Oxford, Great Britain, July 1985.

11. J. van Wijk et al.
MADYMO pedestrian simulations.
Proceedings Pedestrian Impact and Injury Assessment, SAE, Detroit, USA, March 1983.

12. E.G. Janssen and J.J. Nieboer
Protection of vulnerable road users in the event of a collision with a passenger car. Part I - Computer simulations.
TNO Road-Vehicles Research Institute, Report no. 754050002/1, Delft, December 1990.

13. J. Harris et al.
Summary of the work of the consortium developing test methods to evaluate the protection afforded to pedestrians by cars (including test proposals).
European Commission Contract No: ETD/89/7750/M1/28, 1991.

Appendix 1

no.	Time of first contact (ms)	Contact with bodypart	Normal imp. velocity (m/s)	Resultant imp. velocity (m/s)	Deformation energy (J)	Effective mass (kg)
1	27.3	upper left leg	6.26	6.33	379	19.34
2	25.3	upper left leg	6.49	6.53	380	18.04
3	28.8	upper left leg	5.91	5.95	406	23.25
4	8.0	upper left leg	9.35	9.36	679	15.53
5	8.2	upper left leg	8.69	8.70	592	15.68
6	8.5	upper left leg	8.08	8.11	538	16.48
7	41.7	upper left leg	6.33	6.84	226	11.28
8	43.0	upper left leg	6.48	6.92	258	12.29
9	44.2	upper left leg	6.46	6.71	300	14.38
10	37.0	upper left leg	4.38	4.95	52	5.42
11	9.2	upper left leg	7.06	7.06	155	6.22
12	59.2	upper left leg	2.78	4.04	5	1.29
13	8.0	upper left leg	9.79	9.80	842	17.57
14	22.0	upper left leg	8.34	8.40	701	20.16
15	35.2	upper left leg	8.83	8.90	608	15.60

Table A.1a Leading-edge impact - responses 50th percentile male.

no.	Impact angle (°)	Impact loc. angle (°)	Total impact angle (°)	Maximum penetration (m)	Max. bend. moment ULL (Nm)
1	81.3	154.1	145	0.082	272
2	83.6	160.4	154	0.076	309
3	83	148.9	142	0.093	330
4	91.9	178.1	180	0.110	446
5	93.2	177.8	181	0.105	540
6	94.9	177.3	182	0.105	674
7	67.8	140.8	119	0.062	362
8	69.6	137.8	117	0.074	209
9	74.4	135.4	120	0.084	180
10	62.3	142.3	115	0.023	752
11	89.4	172.3	172	0.031	942
12	43.5	120.7	74	0.011	713
13	94.4	179.7	184	0.183	397
14	93.0	162.6	166	0.149	196
15	81.4	150.5	142	0.128	161

Table A.1b Leading-edge impact - responses 50th percentile male.

no.	Time of first contact (ms)	Contact with bodypart	Normal imp. velocity (m/s)	Resultant imp. velocity (m/s)	Deformation energy (J)	Effective mass (kg)
1	28.3	upper left leg	7.31	7.35	265	9.92
2	27.0	upper left leg	8.07	8.12	299	9.18
3	29.8	upper left leg	6.33	6.54	259	12.93
4	12.0	upper left leg	8.74	8.76	469	12.28
5	12.3	upper left leg	8.24	8.26	423	12.46
6	12.5	upper left leg	7.95	7.97	365	11.55
7	40.5	lower torso	6.95	8.41	321	13.29
8	41.7	lower torso	7.04	7.61	307	12.39
9	43.0	lower torso	6.66	6.84	226	10.19
10	38.2	upper left leg	4.41	4.60	67	6.89
11	14.0	upper left leg	5.04	5.11	120	9.45
12	56.2	upper left leg	4.06	4.56	54	6.55
13	11.5	lower torso	9.37	11.09	502	11.44
14	22.5	lower torso	9.88	10.04	502	10.29
15	34.8	lower torso	8.79	9.06	294	7.61

Table A.2a Leading-edge impact - responses 5th percentile female.

no.	Impact angle (°)	Impact loc. angle (°)	Total impact angle (°)	Maximum penetration (m)	Max. bend. moment ULL (Nm)
1	83.7	152.4	146	0.069	144
2	83.5	155.3	149	0.083	164
3	104.6	152.3	167	0.047	152
4	93.9	175.8	180	0.111	279
5	93.9	174.5	178	0.107	314
6	94.5	173.9	178	0.100	390
7	55.7	118.2	84	0.057	153
8	67.8	123.7	102	0.049	144
9	103.3	143.0	156	0.059	127
10	73.5	137.8	121	0.027	253
11	99.2	171.3	181	0.040	510
12	62.8	118.0	91	0.023	135
13	57.7	147.1	115	0.098	155
14	79.7	151.8	142	0.082	142
15	104.1	165.5	180	0.087	136

Table A.2b Leading-edge impact - responses 5th percentile female.

no.	Time of first contact (ms)	Contact with bodypart	Normal imp. velocity (m/s)	Resultant imp. velocity (m/s)	Deformation energy (J)	Effective mass (kg)
1	33.3	spine	4.58	5.20	30.75	2.93
2	28.0	spine	8.04	8.40	136.50	4.22
3	41.2	upper torso	5.34	5.34	43.23	3.03
4	16.3	spine	9.28	9.70	95.04	2.21
5	16.5	spine	8.37	8.54	66.37	1.89
6	17.5	spine	6.95	6.95	35.78	1.48
7	44.7	upper torso	8.88	9.22	149.60	3.79
8	49.5	upper torso	7.23	7.26	81.31	3.11
9	45.7	shoulder	7.86	8.44	131.40	4.25
10	49.5	spine	4.06	4.18	34.88	4.23
11	17.0	upper leg left	6.63	6.94	61.85	2.81
12	63.7	upper torso	4.93	5.79	0.00	0.00
13	18.5	upper torso	7.05	8.18	126.34	5.08
14	29.0	upper torso	8.84	9.06	179.40	4.59
15	38.7	shoulder	10.55	10.82	191.70	3.44

Tabel A.3a Leading-edge impact - responses six-year-old child.

no.	Impact angle (°)	Impact loc. angle (°)	Total impact angle (°)	Maximum penetration (m)
1	118.3	159.7	188	0.018
2	106.8	160.4	177	0.044
3	89.5	109.0	109	0.021
4	73.1	149.3	132	0.034
5	78.5	150.1	139	0.027
6	90.0	149.6	150	0.019
7	74.4	124.1	109	0.052
8	95.4	128.1	134	0.030
9	111.3	126.2	148	0.048
10	76.0	118.6	105	0.019
11	67.4	142.2	120	0.020
12	58.3	95.2	64	0.014
13	59.5	134.5	104	0.041
14	77.3	142.8	130	0.055
15	77.3	109.1	96	0.037

Tabel A.3b Leading-edge impact - responses six-year-old child.